

Perovskites for CO₂ Reduction

Subjects: [Electrochemistry](#)

Contributor: Mina Ahmadi-Kashani , Mahmoud Zendeheel , Luigi Schirone , Mohammad Mahdi Abolhasani , Narges Yaghoobi Nia

Due to their outstanding operational and compositional properties, perovskite-based structures have already been studied as an important class of solid-state components for electrochemical (EC), photoelectrochemical (PEC), and photovoltaic–electrochemical (PV-EC) CO₂ reduction, showing great potential in their catalytic activity and device stability and with a promising window for further technological developments.

perovskite

electrochemical

photoelectrochemical

photovoltaic–electrochemical

1. Introduction

Anthropogenic CO₂ emissions have increased significantly as a result of the extensive use of fossil fuels for energy generation. The International Energy Agency estimates that around 81% of the world's energy consumption is met by fossil fuels. The entire energy demand is anticipated to increase to 24–26 TW by 2040, with CO₂ emissions averaging 37–44 Gt annually [1]. It is critical to close the carbon cycle because this is one of the biggest issues facing our civilization. Global warming, glacier melting, and ocean acidification are just a few of the environmental issues brought on by an excessive amount of CO₂ in the atmosphere. These issues have a long-term negative impact on both humans' wellbeing and the health of the planet's ecosystem [2][3]. As a result of these serious problems, developing progressive technologies for CO₂ capture, utilization, and storage (CCUS) is becoming increasingly necessary in the twenty-first century. Accordingly, we need to focus more on renewable energy sources and relevant transition technologies. Renewable energy systems such as solar and wind power can be considered the main sources of electricity supply, and the rates of electrical energy produced from them is estimated to be comparable to conventional coal generation [4][5]. As essential operational resources for the exploitation and storing of renewable energy, electrocatalytic carbon dioxide reduction reactions can be performed to capture and activate stable CO₂ molecules via electrochemical (EC), photovoltaic–electrochemical (PV-EC), or photoelectrochemical (PEC) catalysis, resulting in the creation of a number of products such as methane, methanol, ethanol, carbon monoxide, formic acid, and so on [6][7]. Electrocatalysis is a catalytic process that involves the conversion of electrical energy into chemical energy through the use of electricity [8]. PV-EC consists of an integration between photovoltaic (PV) and electrochemical (EC) systems due to the capture of the incident photon and the use of the generated photovoltage for synthesizing the necessary carbon-based chemicals when fed with CO₂. Meanwhile, the photoelectrochemical (PEC) technique, which uses a semiconductor light collector and is integrated with an electrochemical catalyst in a device stack, is an outstanding method for CO₂ reduction, using sunlight as an energy supply [9][10]. Compared with conventional high-temperature thermal conversion, electrochemical CO₂ reduction using sustainable energy sources is more favorable because of its mild functional

situations [11]. Electro-CO₂ reduction (CO₂ER) offers an attractive way to convert CO₂ into additional chemicals under standard ambient atmospheric temperature and pressure (SATP) conditions, and it can be simply joined with renewable energy sources like wind and solar power, providing a “green” path to carbon recycling [12]. However, because of the slow reaction mechanism of inert CO₂ molecules, which initiates a competitive process (hydrogen evolution reaction; HER) and leads to low faradaic efficiency in aqueous solutions, the practical application of direct CO₂ER has been seriously delayed [13]. In addition, due to the multiple proton–electron transfer mechanisms, CO₂ER products are usually very complex, leading to excessive costs for separation and purification [14].

As for CO₂ER, while many metallic (e.g., Ag, Au, Pd, Cu, Co, Sn) and non-metallic (e.g., N-doped graphene, carbon nanotubes) catalysts have been investigated and shown to have significant catalytic activity, their performance is much lower than expected [15]. For example, Sn derivatives have received a lot of attention because of the selectivity of their formed products, but they usually suffer from limited reaction selectivity and activity [13]. Therefore, using efficient catalysts with selectivity and acceptable activity is important but also challenging.

In recent decades, perovskites with the general formula ABX₃ have been devoted significant consideration owing to their flexible compositions and diverse properties, and they have found broad applications in the fields of electronics, photonics, photovoltaics, magnetism, and catalysis [16][17][18][19][20][21], showing a promising potential to reach the best sustainable solution based on the results of their life-cycle assessment (LCA) [22]. Previous studies have shown that the metal–oxygen bonds in the perovskite form the basis for the regulation of its electronic properties, which further affects the surface binding energy [23]. In addition, B (BO₅) surface sites with an asymmetric coordination environment also induce special surface properties for perovskites. The high flexibility in the arrangement and crystal structure of perovskites lead to their tunable electronic structure, with well-defined physical and chemical properties, making them ideal candidates as electrocatalysts for CO₂ reduction [24][25].

2. Structure of Perovskites

Depending on their ability to occupy different cationic and anionic sites, perovskites can present in various forms, including as oxides, sulfides, nitrides, and metal–halides [26]. Perovskites have four dimensionalities, namely 0-D, 1-D, 2-D, and 3-D, which exist in various forms; for example, (a) ABX₃ perovskites (e.g., CH₃NH₃PbI₃, CaTiO₃), (b) A₂BX₄ layered perovskites (e.g., Cs₂PbI₄), (c) A₂BB'X₆ double perovskites (e.g., Sr₂FeMoO₆, Ba₂TiRuO₆), and (d) A₂A'B₂B'X₉ triple perovskites (e.g., La₂SrCo₂FeO₉) [27]. A variety of cation/anion combinations can be employed to create different shapes while maintaining charge neutrality.

2.1. Perovskite Oxides

Several transition metal oxides with the basic chemical formula of ABO₃ belong to the perovskite oxide family, where the 12-fold O-coordinated A-sites and the 6-fold O-coordinated B-sites are occupied by the larger alkali metals or rare-earth cations and the smaller transition metal cations, respectively. The A- and B-sites of perovskite oxides could be substituted by almost 90% of the elements in the periodic table. A common approach to expanding

the perovskite family and adjusting its properties is doping new cations at A and B sites that possibly will lead to a random or well-organized arrangement. These oxides typically are in a cubic structure, but it is possible to display transitions to hexagonal, tetrahedral, orthorhombic, and rhombohedral structures [28]. Structural variations in perovskite oxides can lead to the realization of different magnetic orderings [29]. The appropriate substitution of anions/cations or the doping of these perovskites can create a variety of piezoelectric, ferroelectric, superconducting, catalytic, metallic, and magnetic properties [30]. This wide range of properties allows perovskite oxides to be used in various electronic devices, piezoelectric devices, biosensors, transducers, and actuators [31][32][33]. Owing to their structure flexibility, high stability, distinctive arrangement, ionic conductivity, as well as their electron mobility and redox behavior, perovskite oxides are also used as electrocatalysts in different reactions. In particular, the application of these perovskites in electrocatalysis have following advantages: (1) more stoichiometric regulation and homogeneity are provided at a low cost and in an easy synthetic procedure; (2) modulation of perovskite oxide properties lead to the use of a wide range of substituting components. Despite the extensive use of perovskite oxides in various fields, these compounds face serious challenges. For example, at high temperature, perovskite oxides can easily decompose or react with other materials. This can limit their use in high-temperature processes.

2.2. Metal–Halide Perovskites

Owing to their favorable features such as efficient optoelectronic properties, low cost, and simple synthesis method, metal–halide perovskites can be considered a notable material for next-generation devices [34][35][36]. Metal–halide perovskites have a general formula of ABX₃, where A is a monovalent organic or inorganic cation (e.g., CH₃NH₃⁺, Cs⁺), B is a divalent metal cation (e.g., Pb²⁺), and X is a halide ion. Depending on the cations in the A-site of the perovskite structure, these compounds are divided into organometallic halide perovskites (OHPs) and inorganic halide perovskites (IHPs) [37][38][39][40][41][42]. Metal–halide perovskites display high absorption coefficients and high exciton emission and tunable energy bands at ambient temperature. Also, these perovskites are described as favorite direct-bandgap semiconductor compounds [43][44]. MAPbI₃ and FAPbI₃ are the main types of these perovskites and are the most widely applied materials in photovoltaic applications due to their high absorption coefficient and high electron and hole mobility [45]. In particular, these classes of hybrid metal–halide perovskites are well developed for various scalable solution-based deposition techniques, with a promising pathway toward the sustainable generation of renewable energies [16][46][47][48][49][50]. In spite of their outstanding features, the metal–halide perovskites have serious problems in practical applications because of their lack of stability.

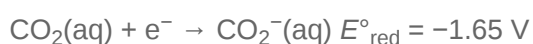
3. Fundamentals of CO₂ Reduction

The electrochemical reduction of CO₂ is a promising and outstanding method that leads to diminishing greenhouse gas emissions by allowing renewable energy storage in different chemical forms. This procedure presents exceptional benefits; for instance, the EC method can employ some environmentally friendly energy sources like solar energy, and it can be carried out at atmospheric temperature and pressure. Meanwhile, through altering the electrolyte and applied voltage, the reaction conditions and products can be controlled [51]. Nevertheless, CO₂ is a

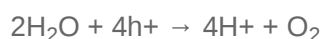
stable and inert linear molecule that requires an appropriate electrocatalyst to assist in breaking the C=O bond. The EC process can yield a diversity of products, including formic acid, formate, oxalic acid or oxalate, carbon monoxide, formaldehyde, methanol, methane, ethanol, ethylene, and other products. Solid-oxide fuel cells (SOFCs) and organic- or inorganic-materials-based electrodes collected with typical electrochemical cells are usually utilized for CO₂ conversion in high-temperature and low-temperature methods, respectively.

SOFC systems reveal a higher selectivity, whereas low-temperature CO₂-reduction reactions usually provide a wide range of products. In addition, low-temperature CO₂-reduction systems involve large overpotentials and, thus, great power requests. In electrochemical CO₂RR, two, four, six, or eight electrons can be transferred.

Nowadays, in order to reduce the disadvantages and promote the benefits of electrochemical and photocatalytic techniques for efficient CO₂ reduction, the combination of both technologies is being investigated. In the photoelectrochemical technique (PEC), which is also known as artificial photosynthesis because it imitates nature's energy cycle, CO₂ reduces into various products at ambient pressure and temperature by harvesting light energy. The PEC CO₂ reduction offers many advantages such as environmental compatibility, great selectivity, economic viability, and the use of solar as a renewable energy source. In PEC systems, photocathodes and anodes are p-type and n-type semiconductors, respectively. Whenever light is illuminated, electrons are formed at the conduction band (CB) and holes are generated at the valence band (VB), leading to band bending at the connection point of the p-type and n-type electrodes. To improve the CO₂ reduction efficiency, band bending is crucial to create discrete electrons and holes at the electrodes and the electrolyte interface [9]. In the PEC CO₂RR process in aqueous solution (pH = 7), various intermediates are produced. The reactions below show the creation of electrons and protons that lead to the formation of various products [52].



Reaction of water and holes:



Formation of hydrogen radicals:



Construction of CO₂ anion radicals:



In the photoelectrochemical procedure, CO₂ can be transformed into different products, such as formaldehyde, carbon monoxide, formic acid, methane, methanol, ethanol, isopropanol, etc.

4. Perovskites for CO₂ Reduction

4.1. Direct Electrochemical CO₂ Reduction

An active and selective CO₂ reduction reaction (CO₂RR) is an important step in recycling excess CO₂ into renewable forms of carbon and building an energy-efficient society. Direct electrochemical CO₂RRs can proceed under ambient conditions and have been extensively studied to understand the fundamentals of catalysis and to develop efficient catalysts for practical applications [53]. Li et al. showed, for the first time, that a Sr₂Fe_{1.5}Mo_{0.5}O_{6-δ} (SFM) ceramic fuel-reforming electrode with a cubic perovskite structure can be used as an electrocatalyst to electrolyze pure CO₂ and convert it into CO without using syn-gases such as H₂ and CO in solid-oxide electrolysis cells [54]. Higher electrochemical efficiencies are demonstrated for single SFM cathodes using pure CO₂ as the feed gas compared with those reported for simple oxide–ceramic electrodes. The electrocatalytic properties of the SFM cathode for CO₂RR in solid-oxide electrolysis cells were tested by supported cells based on the double-layer electrolyte, containing an LSGM (La_{0.9}Sr_{0.1}Ga_{0.8}Mg_{0.2}O_{3-δ}) electrolyte and an LDC (La_{0.4}Ce_{0.6}O_{2-δ}) barrier layer with a thickness of ~230 μm and 5 μm, respectively. Owing to the improved conductivity and greater electrocatalytic activity at raised temperatures, higher current densities and faster CO₂RR rates were obtained by increasing the operational temperature. Applied temperatures of 650, 700, 750, and 800 °C under a voltage of 1.5 V led to current densities of 0.26, 0.33, 0.49, and 0.71 A·cm⁻², respectively. The achieved current density of 0.71 A·cm⁻² was greater than almost all of the reported results for electrolyzing CO₂ using stable oxide electrodes at 800 °C. For CO₂ electrolysis under harsh conditions of pure CO₂ without a shielding gas, a relatively stable efficiency was obtained, and the current density reached above 1 A cm⁻²; furthermore, the faradaic efficiency (FE) was above 95%, which was hardly ever attained in the literature but very desirable for commercial use. By using a SFM–Sm_{0.2}Ce_{0.8}O_{2-δ} composite cathode in 1.5 V and different temperatures of 650, 700, 750, and 800 °C, current densities of 0.40, 0.54, 0.75, and 1.09 A cm⁻² were attained, respectively. Using the SFM–Sm_{0.2}Ce_{0.8}O_{2-δ} composite cathode, the electrocatalytic activity was considerably developed, and the current density showed a growth of about 53.5% in a practical voltage of 1.5 V at 800 °C. These results signified that the SFM ceramics are favorable catalysts for CO₂ electroreduction.

SrSnO₃ nanowires (NWs) with a single 1D nanostructure and cubic perovskite phase have been reported by Pi et al. [55]. An adapted setup of a gas-tight two-chamber with a proton-exchange membrane (PEM) as the separator was designed for electrochemical investigation. An Ag/AgCl electrode, carbon-fiber-paper-modified SrSnO₃ nanowires in the cathodic chamber, and a Pt wire in the anodic chamber were used as the reference electrode (RE), working electrode (WE), and counter electrode (CE), respectively. When applied to CO₂ER catalysis, these prepared perovskite NWs show outstanding selectivity and catalytic activity in formate production, with a high FE (~80%) and remarkable current density over a wide potential range, making them outstanding electrocatalysts for

the CO₂ electroreduction to formate. Consequently, great selectivity (~80%), a large current density (21.6 mA cm⁻²), and a notable durability of at least 10 h were obtained, making a new class of perovskite NWs with potential applications for CO₂ER and beyond. In comparison, bulk SrSnO₃ and SnO₂ nanoparticles (NPs) show very low activity and/or selectivity for CO₂ER.

Various nanostructures based on transition-metal nitrides have been examined for electroreduction reactions; however, a very limited number of these materials have been verified for CO₂ reduction reactions. For instance, Ni₃N was employed for the CO₂ reduction to CO [56]. Yin et al. prepared perovskites based on copper (I) nitride (Cu₃N) nanocubes as a new catalyst for the selective CO₂ reduction to ethylene (C₂H₄) under ambient conditions [57]. These samples were synthesized by the nitridation of copper (II) hydroxide nanowires and were converted into multigrain nanowires to prove their great CO₂ reduction selectivity toward C₂ products, possibly due to the semiconductor properties of Cu₃N. These samples, with perovskite-related ReO₃ structures, can convert CO₂ into ethylene with a faradaic efficiency of about 60% and a Cu mass activity of around 34 A/g in a 0.1 M KHCO₃ electrolyte solution at -1.6 V compared with a reversible hydrogen electrode (RHE). Notably, in the products of the gas phase with a molar ratio of >2000 for C₂H₄/CH₄, the Cu₃N catalyst suspends CH₄ formation, and the highest selectivity is realized for CO₂RR by Cu-based catalysis.

Two bismuth-based halide perovskite composites, Cs₃Bi₂Br₉/C and Cs₂AgBiBr₆/C, were prepared for electrochemical CO₂ reduction to HCOOH by Wang et al. [58]. They carried out the electrochemical analyses in acidic media (pH = 2.5) and could directly convert intermediates to formic acid instead of formate. In acidic electrolysis, the two Cs₃Bi₂Br₉/C and Cs₂AgBiBr₆/C composites can successfully inhibit structural degradation. A great FE of 92% at -0.95 V vs. RHE with a current density (*j*_{HCOOH}) of 133.7 mAcm⁻² was obtained by Cs₃Bi₂Br₉/C, while the Cs₂AgBiBr₆/C show a lower FE (68%) at -1.15 V vs. RHE. More investigation and analyses confirm that the existence of more Bi atoms in Cs₃Bi₂Br₉ is a crucial factor to more favorably generate OCHO* intermediates than Cs₂AgBiBr₆/C, accelerating the fabrication of HCOOH. Moreover, at -0.95 V over 20 h of electrolysis, for Cs₃Bi₂Br₉/C, the current density and FE (~92%) showed no evident decline, while the FE of HCOOH in Cs₂AgBiBr₆/C clearly deteriorated from 68% to 50% at -1.15 V after 10 h. The difference in stability between the two composites could be due to the faster charge transfer and faster increase in the CO₂ conversion ratio for Cs₃Bi₂Br₉ than Cs₂AgBiBr₆, leading to a reduction in the degradation effect and an enhancement in durability in an aqueous electrolyte.

A nanosized LaInO₃ perovskite electrocatalyst was effectively prepared by a simple hydrothermal-calcination method and applied in the electrocatalytic reduction of CO₂ to formate by Zhu et al. [59]. This synthesized electrocatalyst displayed superb activity and excellent selectivity in the CO₂RR. In an aqueous electrolyte solution, CO₂ has low solubility, so its reduction reaction is rigorously restricted in the H-cell, and the current density was very low. So, the flow cell was applied to carry out the CO₂RR. Thus, to solve the problem of solubility and the inadequate mass transfer of CO₂ in an aqueous solution, a suitable setup was designed by the CO₂ diffusion and electrolyte flow-channel-flanked gas-diffusion electrode. The results showed that the current density and faradaic efficiency of LaInO₃ in the flow cell was higher than in the H-cell. Electrochemical tests showed that the FE of

formate reached up 91.4% (−1.1 V vs. RHE) and the current density of formate was 116.8 mA cm^{−2} (−1.1 V vs. RHE).

4.2. Photoelectrochemical CO₂ Reduction

Making advances in electrocatalysts and photoelectrocatalytic systems for the selective and efficient production of a target product is a substantial challenge [60][61][62]. Indeed, perovskite structures with interesting photoconversion and redox properties are always interesting for photoelectrochemical concepts. An In_{0.4}Bi_{0.6} alloy-coated CH₃NH₃PbI₃-based photocathode has been demonstrated to produce selective CO₂ reduction with nearly 100% faradaic efficiency (FE) for formic acid production in aqueous solution by Chen et al. [63]. Their examinations revealed that In_{0.4}Bi_{0.6} and In_{0.6}Bi_{0.2}Sn_{0.2} alloys led to more electrocatalytic activity for the selective production of HCOOH as a result of the presence of the In₅Bi₃ phases. The HCOO*, as the intermediate in this procedure, was better stabilized on the In₅Bi₃ phases than on other alloys. At an applied voltage of −1.2 to −1.3 V versus RHE, the highest FE (95–98%) for the production of HCOOH was achieved by the In_{0.6}Bi_{0.2}Sn_{0.2} and In_{0.4}Bi_{0.6} alloys. Next, a favorable method that included coating the perovskite halide with an In_{0.4}Bi_{0.6} alloy was used. With the In_{0.4}Bi_{0.6}/CH₃NH₃PbI₃ photocathode, at a low applied potential of −0.52 V vs. RHE under AM 1.5G irradiation, almost 100% FE for formic acid formation could be attained, signifying a 680 mV positive shift relative to the potential detected for the In_{0.4}Bi_{0.6} electrode. At −0.6 V vs. RHE, the faradaic efficiency remained at nearly 100% for at least 1.5 h, and a photo-assisted electrocatalysis efficiency of 7.2% was determined. This photoelectrocatalyst showed a high selectivity for CO₂ reduction to HCOOH.

LSV analysis was applied to examine the samples for their PEC performances in a cell containing propylene carbonate solution saturated with CO₂ in 0.1 M tetrabutyl ammonium hexafluorophosphate (TBAPF₆). Compared with the CH₃NH₃PbBr₃ quantum dots, GO/CH₃NH₃PbBr₃ showed an increase in photocurrents for the photoelectrochemical CO₂ reduction, as the maximum variation of photocurrent was observed at ca. −0.6 V. The photocurrent response of the as-synthesized samples was investigated at −0.6 V. This voltage was selected from the LSV results. An increase in the photocurrent response was observed for GO/CH₃NH₃PbBr₃, while CH₃NH₃PbBr₃ showed a decaying photocurrent, suggesting that graphene oxide acts as a stabilizer to preserve CH₃NH₃PbBr₃ QDs. Graphene oxide can protect CH₃NH₃PbBr₃ quantum dots against degradation by organic solvents and can also act as a charge-transfer intermediate to efficiently distinguish generated electrons and holes. The as-prepared catalyst exhibits an outstanding yield for CO₂ conversion to CO (1.05 μmol cm^{−2} h^{−1}). The chronoamperometric analysis was applied to examine the effect of GO on the stability of CH₃NH₃PbBr₃. The photocurrent of CH₃NH₃PbBr₃ remained stable for about 1800 s. After introducing GO, the photocathode produced a long photocurrent for about 6000 s because of the protective effect of GO.

A PEC system based on a Au-decorated ZnO@ZnTe@CdTe photocathode and CH₃NH₃PbI₃ perovskite tandem cell has been verified by Jang et al. as an unbiased solar-driven CO₂ reduction to CO [64]. The designed cell disclosed a stable efficiency of solar-to-CO of above 0.35% with a faradaic efficiency of over 80% and a solar-to-fuel efficiency of more than 0.43%, with H₂ as a byproduct. This PEC cell showed the selective CO creation from CO₂ reduction using an operative photocathode–perovskite tandem device working in sunlight without an exterior

bias. The overpotential was decreased by the ternary photocathode, and the CH₃NH₃PbI₃ perovskite generated a voltage that is sufficient to initiate the reduction of CO₂ without an exterior bias.

4.3. Photovoltaic–Electrochemical CO₂ Reduction

Artificial photosynthesis, a technological device that uses solar irradiation as an energy source and water as an electron source to convert carbon dioxide into energy-dense organic compounds (fuels or other carbons for the chemical industry), is attractive in specific contexts [65]. This can be achieved in an integrated cell by using photovoltaic (PV) cells to supply photoelectrons and holes to be used in an electrochemical cell (EC) to oxidize water at the anode and to reduce carbon dioxide at the cathode, creating a PV-EC reference system to reduce CO₂ to fuels. The PV-EC systems can be classified into two general configurations, namely monolithic and polyolithic. In a monolithic configuration, the junction terminals of the photovoltaic cell is directly connected to the anode and cathode of the EC unit, and the direct-circuit (DC) photogenerated power is designed to be used in the electrocatalytic process without any external electrical connections and/or inversion, while in a polyolithic configuration, the PV and EC cells work separately, and the electrical power of the PV cell can be used in the electrochemical cell usually after a DC/DC inversion. Generally, the polyolithic PV-EC has significantly better controllability of product selectivity, e.g., increasing the applied voltage via the series connection of PV modules and easier matching of the operating current by using certain ratios of the PV and EC areas.

Huan et al. provided a new catalyst for CO₂ conversion to hydrocarbons, which exhibited a faradaic yield of 62% in product generation [66]. This three-layer catalyst contains a metal Cu core protected by layers of CuO and Cu₂O. Remarkably, over a 60 min electrolysis at -0.95 V versus RHE, the structure of the CuO cathode changed. When joined with an advanced, low-cost perovskite photovoltaic minimodule, this PV-EC device achieves a solar-to-fuel value of 2.3% by combining it with a mini-module perovskite photovoltaic device recognized using two sequences of three perovskite photovoltaics with an active area of 0.25 cm² coupled in parallel, offering a yardstick for PV-EC systems that includes plentiful earth-abundant elements. To examine the CO₂-reduction performance on this system, current–voltage measurements of the modules were applied, which exposed a high photo-to-current efficiency (17.5%) at 2.45 V and 10.0 mA. A constant current of 6.0 ± 0.2 mA with a current density of ~18 mA·cm⁻² and a potential of 2.8 ± 0.02 (V) were proved by the connection of both systems. Over a 50 min electrolysis by using the gas chromatography (GC) technique and analyzing the reduction products, it was shown that the PV-EC catalyst generates a steady current.

5. Conclusions

The conversion of CO₂ to added-value chemicals or fuels is an attractive strategy for storing such a renewable source of energy into the form of chemical energy. The catalysis technology has received more and more attention for such a concept. Therefore, in parallel to more developed systems for electrochemical water splitting, the utility of innovative and advanced catalysts to develop critical performance factors, e.g., durability, conversion efficiency, and energy/power densities, must be explored in the specific concept of the CO₂RR. To achieve this purpose, the scientific community has been working on the construction of new materials that allow the design of advanced

electrode systems for efficient CO₂ capture and reduction. Recently, perovskite-based catalysts have drawn a growing interest in various sectors from renewable energy to environmental processes. Perovskite oxides have shown more potential in EC CO₂RRs because of their oxygen vacancy sites and lattice distortions, which create more active sites for electrochemical CO₂ reduction. Moreover, perovskite oxides have more stability under harsh conditions like high temperature and can be used for solid-oxide fuel cells. Due to the presence of halide ions, halide perovskites show higher absorption coefficients and have more carrier mobilities, which make them more suitable for PEC and PV-EC CO₂ reduction [67][68]. To achieve outstanding perovskite-based electrocatalysts, there are various strategies available, including developing the intrinsic activity and increasing available active sites by defect engineering on the perovskite surface, crystal structure regulation, tuning the electrical conductivity and synthesis process, and surface modification. High electron transfer of perovskites leads to the reduction of ohmic losses and the evolution of active sites, developing electrocatalytic performance. To increase electronic conductivity, some strategies such as using electrically conductive materials and doping agents are beneficial.

References

1. Zhang, S.; Jing, X.; Wang, Y.; Li, F. Towards Carbon-Neutral Methanol Production from Carbon Dioxide Electroreduction. *ChemNanoMat* 2021, 7, 728–736.
2. Wu, H.; Yuan, Y.; Chen, Y.; Lv, D.; Tu, S.; Wu, Y.; Li, Z.; Xia, Q. Highly Efficient Capture of Postcombustion Generated CO₂ through a Copper-Based Metal-Organic Framework. *Energy Fuels* 2021, 35, 610–617.
3. Zhang, S.; Kang, P.; Meyer, T.J. Nanostructured tin catalysts for selective electrochemical reduction of carbon dioxide to formate. *J. Am. Chem. Soc.* 2014, 136, 1734–1737.
4. Zheng, Y.; Wang, S.; Pan, Z.; Yin, B. Electrochemical CO₂ reduction to CO using solid oxide electrolysis cells with high-performance Ta-doped bismuth strontium ferrite air electrode. *Energy* 2021, 228, 120579.
5. Zhang, S.; Fan, Q.; Xia, R.; Meyer, T.J. CO₂ Reduction: From Homogeneous to Heterogeneous Electrocatalysis. *Acc. Chem. Res.* 2020, 53, 255–264.
6. Li, Y.; Sun, Q. Recent Advances in Breaking Scaling Relations for Effective Electrochemical Conversion of CO₂. *Adv. Energy Mater* 2016, 6, 1600463.
7. Aresta, M.; Dibenedetto, A. Utilisation of CO₂ as a chemical feedstock: Opportunities and challenges. *Dalt. Trans.* 2007, 28, 2975–2992.
8. Whipple, D.T.; Kenis, P.J.A. Prospects of CO₂ utilization via direct heterogeneous electrochemical reduction. *J. Phys. Chem. Lett.* 2010, 1, 3451–3458.
9. Creissen, C.E.; Fontecave, M. Solar-Driven Electrochemical CO₂ Reduction with Heterogeneous Catalysts. *Adv. Energy Mater.* 2021, 11, 2002652.

10. Bin, A.R.; Yusoff, M.; Jang, J. Highly efficient photoelectrochemical water splitting by a hybrid tandem perovskite solar cell. *Chem. Commun.* 2016, 52, 5824–5827.
11. Zhu, D.D.; Liu, J.L.; Qiao, S.Z. Recent Advances in Inorganic Heterogeneous Electrocatalysts for Reduction of Carbon Dioxide. *Adv. Mater.* 2016, 28, 3423–3452.
12. Kumar, B.; Atla, V.; Brian, J.P.; Kumari, S.; Nguyen, T.Q.; Sunkara, M.; Spurgeon, J.M. Reduced SnO₂ Porous Nanowires with a High Density of Grain Boundaries as Catalysts for Efficient Electrochemical CO₂-into-HCOOH Conversion. *Angew. Chem. Int. Ed.* 2017, 56, 3645–3649.
13. Gu, J.; Héroguel, F.; Luterbacher, J.; Hu, X. Densely Packed, Ultra Small SnO Nanoparticles for Enhanced Activity and Selectivity in Electrochemical CO₂ Reduction. *Angew. Chem.* 2018, 130, 2993–2997.
14. Liu, Y.; Chen, S.; Quan, X.; Yu, H. Efficient Electrochemical Reduction of Carbon Dioxide to Acetate on Nitrogen-Doped Nanodiamond. *J. Am. Chem. Soc.* 2015, 137, 11631–11636.
15. Wu, J.; Yadav, R.M.; Liu, M.; Sharma, P.P.; Tiwary, C.S.; Ma, L.; Zou, X.; Zhou, X.D.; Yakobson, B.I.; Lou, J.; et al. Achieving highly efficient, selective, and stable CO₂ reduction on nitrogen-doped carbon nanotubes. *ACS Nano* 2015, 9, 5364–5371.
16. Zendehtdel, M.; Yaghoobi Nia, N.; Paci, B.; Generosi, A.; Di Carlo, A. Zero-Waste Scalable Blade-Spin Coating as Universal Approach for Layer-By-Layer Deposition of 3D/2D Perovskite Films in High Efficiency Perovskite Solar Modules. *Sol. RRL* 2021, 6, 2100637.
17. Yaghoobi Nia, N.; Saranin, D.; Palma, A.L.; Di Carlo, A. Perovskite solar cells. In *Solar Cells and Light Management*; Elsevier: Amsterdam, The Netherlands, 2020; pp. 163–228.
18. Zhang, H.T.; Park, T.J.; Islam, A.N.M.N.; Tran, D.S.J.; Manna, S.; Wang, Q.; Mondal, S.; Yu, H.; Banik, S.; Cheng, S.; et al. Reconfigurable perovskite nickelate electronics for artificial intelligence. *Science* 2022, 375, 533–539.
19. Sutherland, B.R.; Sargent, E.H. Perovskite photonic sources. *Nat. Photonics* 2016, 10, 295–302.
20. Tofanello, A.; Freitas, A.L.M.; de Queiroz, T.B.; Bonadio, A.; Martinho, H.; Souza, J.A. Magnetism in a 2D Hybrid Ruddlesden–Popper Perovskite through Charge Redistribution Driven by an Organic Functional Spacer. *J. Phys. Chem. Lett.* 2022, 13, 1406–1415.
21. Hwang, J.; Rao, R.R.; Giordano, L.; Katayama, Y.; Yu, Y.; Shao-Horn, Y. Perovskites in catalysis and electrocatalysis. *Science* 2017, 358, 751–756.
22. Zendehtdel, M.; Yaghoobi Nia, N.; Yaghoobinia, M. Emerging Thin Film Solar Panels. In *Reliability and Ecological Aspects of Photovoltaic Modules*; IntechOpen: London, UK, 2020.
23. Sun, H.; Dai, J.; Zhou, W.; Shao, Z. Emerging Strategies for Developing High-Performance Perovskite-Based Materials for Electrochemical Water Splitting. *Energy Fuels* 2020, 34, 10547–10567.

24. Liang, J.; Chen, D.; Yao, X.; Zhang, K.; Qu, F.; Qin, L.; Huang, Y.; Li, J. Recent Progress and Development in Inorganic Halide Perovskite Quantum Dots for Photoelectrochemical Applications. *Small* 2020, 16, 1903398.
25. Zhao, B.; Yan, B.; Jiang, Z.; Yao, S.; Liu, Z.; Wu, Q.; Ran, R.; Senanayake, S.D.; Weng, D.; Chen, J.G. High selectivity of CO₂ hydrogenation to CO by controlling the valence state of nickel using perovskite. *Chem. Commun.* 2018, 54, 7354–7357.
26. Goel, P.; Sundriyal, S.; Shrivastav, V.; Mishra, S.; Dubal, D.P.; Kim, K.H.; Deep, A. Perovskite materials as superior and powerful platforms for energy conversion and storage applications. *Nano Energy* 2021, 80, 105552.
27. Yin, W.J.; Weng, B.; Ge, J.; Sun, Q.; Li, Z.; Yan, Y. Oxide perovskites, double perovskites and derivatives for electrocatalysis, photocatalysis, and photovoltaics. *Energy Environ. Sci.* 2019, 12, 442–462.
28. Li, X.; Zhao, H.; Liang, J.; Luo, Y.; Chen, G.; Shi, X.; Lu, S.; Gao, S.; Hu, J.; Liu, Q.; et al. A-site perovskite oxides: An emerging functional material for electrocatalysis and photocatalysis. *J. Mater. Chem. A* 2021, 9, 6650–6670.
29. Porta, P.; De Rossi, S.; Faticanti, M.; Minelli, G.; Pettiti, I.; Lisi, L.; Turco, M. Perovskite-Type Oxides: I. Structural, Magnetic, and Morphological Properties of LaMn_{1-x}Cu_xO₃ and LaCo_{1-x}Cu_xO₃ Solid Solutions with Large Surface Area. *J. Solid State Chem.* 1999, 146, 291–304.
30. Wei, W.J.; Li, C.; Li, L.S.; Tang, Y.Z.; Jiang, X.X.; Lin, Z.S. Phase transition, optical and dielectric properties regulated by anion-substitution in a homologous series of 2D hybrid organic–inorganic perovskites. *J. Mater. Chem. C* 2019, 7, 11964–11971.
31. Song, K.W.; Lee, K.T. Characterization of Ba_{0.5}Sr_{0.5}M_{1-x}FexO_{3-δ} (M = Co and Cu) perovskite oxide cathode materials for intermediate temperature solid oxide fuel cells. *Ceram. Int.* 2012, 38, 5123–5131.
32. Devi, S.; Taxak, V.B.; Chahar, S.; Dalal, M.; Dalal, J.; Hooda, A.; Khatkar, A.; Malik, R.K.; Khatkar, S.P. Crystal chemistry and optical analysis of a novel perovskite type SrLa₂Al₂O₇:Sm³⁺ nanophosphor for white LEDs. *Ceram. Int.* 2019, 45, 15571–15579.
33. Zhang, L.; Hu, J.; Song, P.; Qin, H.; Jiang, M. Electrical properties and ethanol-sensing characteristics of perovskite La_{1-x}PbxFeO₃. *Sens. Actuators B Chem.* 2006, 114, 836–840.
34. Bhat, A.A.; Khandy, S.A.; Islam, I.; Tomar, R. Optical, electrochemical and photocatalytic properties of cobalt doped CsPbCl₃ nanostructures: A one-pot synthesis approach. *Sci. Rep.* 2021, 11, 16473.
35. Islam, I.; Khandy, S.A.; Zaman, M.B.; Hafiz, A.K.; Siddiqui, A.M.; Chai, J.-D. Growth and characterization of crystalline BaSnO₃ perovskite nanostructures and the influence of heavy Mn

- doping on its properties. *J. Alloys Compd.* 2021, 867, 158900.
36. Khandy, S.A.; Vaid, S.G.; Islam, I.; Hafiz, A.K.; Chai, J.-D. Understanding the stability concerns and electronic structure of CsYbX₃ (X=Cl,Br) halidoperovskites for optoelectronic applications. *J. Alloys Compd.* 2021, 867, 158966.
37. Babu, R.; Giribabu, L.; Singh, S.P. Recent Advances in Halide-Based Perovskite Crystals and Their Optoelectronic Applications. *Cryst. Growth Des.* 2018, 18, 2645–2664.
38. Yaghubinia, M.; Ebnali, M.; Zendehtdel, M.; Yaghoubinia, M. Improvement of perovskite solar cells photovoltaic performance by localized surface plasmon effect of silver-alumina core-shell nanoparticles. In *Proceedings of the PHOTOPTICS 2016-Proceedings of the 4th International Conference on Photonics, Optics and Laser Technology, Rome, Italy, 27–29 February 2016.*
39. Di Carlo, A.; Yaghoobi Nia, N.; Zendehtdel, M.; Agresti, A.; Pescetelli, S.; Vesce, L.; Castriotta, L.A.; Matteocci, F.; Di Giacomo, F.; Saranin, D.; et al. Halide perovskite modules and panels. In *Proceedings of the nanoGe Spring Meeting 2022; Fundació Scito: València, Spain, 2022.*
40. Yaghoobi Nia, N.; Zendehtdel, M.; Abdi-Jalebi, M.; Castriotta, L.A.; Kosasih, F.U.; Lamanna, E.; Abolhasani, M.M.; Zheng, Z.; Andaji-Garmaroudi, Z.; Asadi, K.; et al. Beyond 17% stable perovskite solar module via polaron arrangement of tuned polymeric hole transport layer. *Nano Energy* 2021, 82, 105685.
41. Schmidt, L.C.; Pertegás, A.; González-Carrero, S.; Malinkiewicz, O.; Agouram, S.; Espallargas, G.M.; Bolink, H.J.; Galian, R.E.; Pérez-Prieto, J. Nontemplate synthesis of CH₃NH₃PbBr₃ perovskite nanoparticles. *J. Am. Chem. Soc.* 2014, 136, 850–853.
42. Yaghoobi Nia, N.; Lamanna, E.; Zendehtdel, M.; Palma, A.L.; Zurlo, F.; Castriotta, L.A.; Di Carlo, A. Doping Strategy for Efficient and Stable Triple Cation Hybrid Perovskite Solar Cells and Module Based on Poly(3-hexylthiophene) Hole Transport Layer. *Small* 2019, 15, 1904399.
43. Hao, F.; Stoumpos, C.C.; Cao, D.H.; Chang, R.P.H.; Kanatzidis, M.G. Lead-free solid-state organic–inorganic halide perovskite solar cells. *Nat. Photonics* 2014, 8, 489–494.
44. Sardashti, M.K.; Zendehtdel, M.; Yaghoobi Nia, N.; Karimian, D.; Sheikhi, M. High Efficiency MAPbI₃ Perovskite Solar Cell Using a Pure Thin Film of Polyoxometalate as Scaffold Layer. *ChemSusChem* 2017, 10, 3773–3779.
45. Li, Y.F.; Chou, S.Y.; Huang, P.; Xiao, C.; Liu, X.; Xie, Y.; Zhao, F.; Huang, Y.; Feng, J.; Zhong, H.; et al. Stretchable Organometal-Halide-Perovskite Quantum-Dot Light-Emitting Diodes. *Adv. Mater.* 2019, 31, 1807516.
46. Navazani, S.; Yaghoobi Nia, N.; Zendehtdel, M.; Shokuhfar, A.; Di Carlo, A. Fabrication of high efficiency, low-temperature planar perovskite solar cells via scalable double-step crystal engineering deposition method fully out of glove box. *Sol. Energy* 2020, 206, 181–187.

47. Ermanova, I.; Yaghoobi Nia, N.; Lamanna, E.; Di Bartolomeo, E.; Kolesnikov, E.; Luchnikov, L.; Di Carlo, A. Crystal Engineering Approach for Fabrication of Inverted Perovskite Solar Cell in Ambient Conditions. *Energies* 2021, 14, 1751.
48. Castriotta, L.A.; Zendeudel, M.; Yaghoobi Nia, N.; Leonardi, E.; Löffler, M.; Paci, B.; Generosi, A.; Rellinghaus, B.; Di Carlo, A. Reducing Losses in Perovskite Large Area Solar Technology: Laser Design Optimization for Highly Efficient Modules and Mini Panels. *Adv. Energy Mater* 2022, 12, 2103420.
49. Zhang, H.; Darabi, K.; Yaghoobi Nia, N.; Krishna, A.; Ahlawat, P.; Guo, B.; Almalki, M.H.S.; Su, T.S.; Ren, D.; Bolnykh, V.; et al. A universal co-solvent dilution strategy enables facile and cost-effective fabrication of perovskite photovoltaics. *Nat. Commun.* 2022, 13, 89.
50. Yaghoobi Nia, N.; Giordano, F.; Zendeudel, M.; Cinà, L.; Palma, A.L.; Medaglia, P.G.; Zakeeruddin, S.M.; Grätzel, M.; Di Carlo, A. Solution-based heteroepitaxial growth of stable mixed cation/anion hybrid perovskite thin film under ambient condition via a scalable crystal engineering approach. *Nano Energy* 2020, 69, 104441.
51. Ochedi, F.O.; Liu, D.; Yu, J.; Hussain, A.; Liu, Y. Photocatalytic, electrocatalytic and photoelectrocatalytic conversion of carbon dioxide: A review. *Environ. Chem. Lett.* 2021, 19, 941–967.
52. Kumaravel, V.; Bartlett, J.; Pillai, S.C. Photoelectrochemical Conversion of Carbon Dioxide (CO₂) into Fuels and Value-Added Products. *ACS Energy Lett.* 2020, 5, 486–519.
53. Chen, K.; Qi, K.; Zhou, T.; Yang, T.; Zhang, Y.; Guo, Z.; Lim, C.K.; Zhang, J.; Žutić, I.; Zhang, H.; et al. Water-Dispersible CsPbBr₃ Perovskite Nanocrystals with Ultra-Stability and its Application in Electrochemical CO₂ Reduction. *Nano-Micro Lett.* 2021, 13, 172.
54. Li, Y.; Chen, X.; Yang, Y.; Jiang, Y.; Xia, C. Mixed-Conductor Sr₂Fe_{1.5}Mo_{0.5}O_{6-δ} as Robust Fuel Electrode for Pure CO₂ Reduction in Solid Oxide Electrolysis Cell. *ACS Sustain. Chem. Eng.* 2017, 5, 11403–11412.
55. Pi, Y.; Guo, J.; Shao, Q.; Huang, X. All-inorganic SrSnO₃ perovskite nanowires for efficient CO₂ electroreduction. *Nano Energy* 2019, 62, 861–868.
56. Hou, P.; Wang, X.; Wang, Z.; Kang, P. Gas Phase Electrolysis of Carbon Dioxide to Carbon Monoxide Using Nickel Nitride as the Carbon Enrichment Catalyst. *ACS Appl. Mater. Interfaces* 2018, 10, 38024–38031.
57. Yin, Z.; Yu, C.; Zhao, Z.; Guo, X.; Shen, M.; Li, N.; Muzzio, M.; Li, J.; Liu, H.; Lin, H.; et al. Cu₃N nanocubes for selective electrochemical reduction of CO₂ to ethylene. *Nano Lett.* 2019, 19, 8658–8663.
58. Wang, Y.; Wang, C.; Wei, Y.; Wei, F.; Kong, L.; Feng, J.; Lu, J.-Q.; Zhou, X.; Yang, F. Efficient and Selective Electroreduction of CO₂ to HCOOH over Bismuth-Based Bromide Perovskites in Acidic

- Electrolytes. *Chem. Eur. J.* 2022, 28, e202201832.
59. Zhu, Y.; Zhou, W.; Dong, Z.; Zhang, X.; Chen, Z.; Liu, Z.; Li, F.; Fan, J.; Jiao, M.; Liu, L. Nanosized LaInO₃ perovskite for efficient electrocatalytic reduction of CO₂ to formate. *J. CO₂ Util.* 2023, 68, 102342.
60. Sivula, K.; Van De Krol, R. Semiconducting materials for photoelectrochemical energy conversion. *Nat. Rev. Mater.* 2016, 1, 15010.
61. Sun, H.; Song, S.; Xu, X.; Dai, J.; Yu, J.; Zhou, W.; Shao, Z.; Jung, W. Recent Progress on Structurally Ordered Materials for Electrocatalysis. *Adv. Energy Mater.* 2021, 11, 2101937.
62. Arandiyana, H.; Mofarah, S.S.; Sorrell, C.C.; Doustkhah, E.; Sajjadi, B.; Hao, D.; Wang, Y.; Sun, H.; Ni, B.J.; Rezaei, M.; et al. Defect engineering of oxide perovskites for catalysis and energy storage: Synthesis of chemistry and materials science. *Chem. Soc. Rev.* 2021, 50, 10116–10211.
63. Chen, J.; Yin, J.; Zheng, X.; Ait Ahsaine, H.; Zhou, Y.; Dong, C.; Mohammed, O.F.; Takanebe, K.; Bakr, O.M. Compositionally Screened Eutectic Catalytic Coatings on Halide Perovskite Photocathodes for Photoassisted Selective CO₂ Reduction. *ACS Energy Lett.* 2019, 4, 1279–1286.
64. Jang, Y.J.; Jeong, I.; Lee, J.; Lee, J.; Ko, M.J.; Lee, J.S. Unbiased Sunlight-Driven Artificial Photosynthesis of Carbon Monoxide from CO₂ Using a ZnTe-Based Photocathode and a Perovskite Solar Cell in Tandem. *ACS Nano.* 2016, 10, 6980–6987.
65. Schreier, M.; Héroguel, F.; Steier, L.; Ahmad, S.; Luterbacher, J.S.; Mayer, M.T.; Luo, J.; Grätzel, M. Solar conversion of CO₂ to CO using Earth-abundant electrocatalysts prepared by atomic layer modification of CuO. *Nat. Energy* 2017, 2, 17087.
66. Huan, T.N.; Dalla Corte, D.A.; Lamaison, S.; Karapinar, D.; Lutz, L.; Menguy, N.; Foldyna, M.; Turren-Cruz, S.H.; Hagfeldt, A.; Bella, F.; et al. Low-cost high-efficiency system for solar-driven conversion of CO₂ to hydrocarbons. *Proc. Natl. Acad. Sci. USA* 2019, 116, 9735–9740.
67. Khandy, S.A.; Islam, I.; Kaur, K.; Ali, A.M.; El-Rehim, A.F.A. Electronic structure, stability, photocatalytic and optical properties of new lead-free double perovskites TI₂PtX₆ (X = Cl, Br) for light-harvesting applications. *Mater. Chem. Phys.* 2023, 297, 127293.
68. Bhat, A.A.; Khandy, S.A.; Ali, A.M.; Tomar, R. Photoluminescence Emission Studies on a Lanthanum-Doped Lead Free Double Halide Perovskite, La:Cs₂SnCl₆. *J. Phys. Chem. Lett.* 2023, 14, 5004–5012.

Retrieved from <https://encyclopedia.pub/entry/history/show/120227>